An Easily Removable, wireless Optical Sensing System (EROSS) for the trumpet

Leonardo Jenkins
Electrical and Computer Engineering
University of Victoria
Victoria, BC
leonardo@ece.uvic.ca

Wyatt Page
Electrical Engineering
Massey University
New Zealand
w.h.page@massey.ac.nz

Shawn Trail
Department of Computer Science
University of Victoria
Victoria, BC
trl77@uvic.ca

George Tzanetakis
Department of Computer Science
University of Victoria
Victoria, BC
gtzan@cs.uvic.ca

Peter Driessen
Electrical and Computer Engineering
University of Victoria
Victoria, BC
peter@ece.uvic.ca

ABSTRACT

This paper presents a minimally-invasive, wireless optical sensor system for use with any conventional piston valve acoustic trumpet. It is designed to be easy to install and remove by any trumpeter. Our goal is to offer the extended control afforded by hyperinstruments without the hard to reverse or irreversible invasive modifications that are typically used for adding digital sensing capabilities. We utilize optical sensors to track the continuous position displacement values of the three trumpet valves. These values are transmitted wirelessly and can be used by an external controller. The hardware has been designed to be reconfigurable by having the housing 3D printed so that the dimensions can be adjusted for any particular trumpet model. The result is a low cost, low power, easily replicable sensor solution that offers any trumpeter the ability to augment their own existing trumpet without compromising the instrument's structure or playing technique. The extended digital control afforded by our system is interweaved with the natural playing gestures of an acoustic trumpet. We believe that this seamless integration is critical for enabling effective and musical human computer interaction.

Keywords

hyperinstrument, trumpet, minimally-invasive, gesture sensing, wireless, I^2C

1. INTRODUCTION

Hyperinstruments are expanded acoustic musical instruments that use digital sensors to capture detailed aspects of the performer gestures as well as provide additional expressive capabilities through digital control. They enable the musician to access the diverse possibilities afforded by digital control while at the same time leveraging the skill developed through years of training by professional musicians. Although there are examples of earlier work in this direction, the term "hyperinstrument" was introduced in 1987 through the work of Tod Machover at MIT [9]. Since then, a variety of different hyperinstruments, designed for the main musical instrument families, have been proposed. Early representative examples include: the *Hypercello* (strings) [12], the *Metasaxophone* [1] and *Hyperflute* [11] (winds), and the Cook/Morrill trumpet controller (brass) [3]. Any acoustic instrument can serve as the basis for designing and building a hyperinstrument and the concept has also been applied to non-western instruments such as the sitar [7], and the Gyil african xylophone [14]. Despite the potential of hyperinstruments to enable extended performance techniques, their adoption has been slow and idiosyncratic. We believe that this is mostly due to the following factors: 1) they are expensive custom-made devices that are hard to replicate (typically there is only a single instance in existance); 2) they frequently require invasive modifications to the original acoustic instrument, 3) their operation and maintenance requires significant technical expertise with electronics.

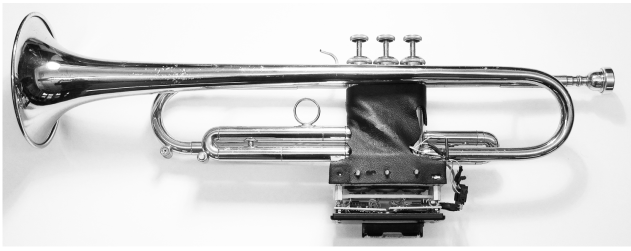

Figure 1: EROSS mounted on a trumpet

The focus of the work presented in this paper is to augment traditional trumpet playing with digital control. There is a long history of approaches that have been proposed to achieve this. The most generic approach is to use external controllers such as foot pedals, knobs, sliders, and keyboards to control digital processes as well as filters/effects on the audio signal produced by the horn. An iconic example of this approach was the use of electric guitar effects by Miles Davis to modify the sound of the trumpet during his electric phase in the 1970s[5]. As any controller can be used for this purpose, this approach provides a very rich set of control possibilities to the trumpet player. In addition,

NIME'13, May 27 – 30, 2013, KAIST, Daejeon, Korea.

it requires no modification to the acoustic instrument other than attaching a microphone to the horn. However, interacting with the controllers is external to the trumpeter's technique. This creates additional cognitive load similar to trying to play two instruments at the same time.

An alternative approach is to directly introduce sensors for digital control on the body of the trumpet making it a hyperinstrument. A good overview of different approaches and sensors that can be used for augmenting the trumpt can be found in the Master thesis of Thibodeau [13]. The pioneering Cook and Morrill trumpet controller [3] was built to create an interface for trumpeter Wynton Marsalis. Sensors on the valves, mouthpiece, and bell enabled fast and accurate pitch detection and provided extended computer control. Another well known example is the *Mutantrumpet*, a hybrid electro-acoustic instrument designed and evolved over many years by composer and inventor Ben Neill [10]. The *Mutantrumpet* started as an acoustic instrument (three trumpets and a trombone combined into a single instrument). In the mid 1980s electronics were integrated to the instrument in collaboration with synthesizer inventor Robert Moog and in the 1990s the instrument was made computer interactive. By attaching the sensors directly on the instrument the digital control is more easily accessible by the player and therefore is more naturally integrated with the traditional way of playing the instrument. However, each instrument is unique, idiosyncratic and custom-made which makes replication and therefore adoption difficult. The modifications to the instrument are extensive (sometimes even radically modifying the original instrument as in the case of the *Mutantrumpt*) and the sensing apparatus is hard to remove if not required. Finally, the detailed design plans and component parts of most augmented trumpets (and hyperinstruments in general) are not publicly available.

Here we present a low-cost, easily removable and minimally invasive optical sensing system (EROSS) that provides continuous control data from the position of the valves on the acoustic trumpet. The housing has been 3D printed making it fully customizable for any standard trumpet. The sensors and housing bracket mount under the valves without obstructing the conventional playing position and the two pieces are connected together via magnets without altering the horn's structure or requiring cumbersome fastening. Our approach has been inspired by the *Electrumpet* [8] which is an enhancement of a normal trumpet with a variety of electronic sensors and buttons. The *Electrumpet* can be attached and detached to any Bb trumpet. It is common for trumpet players to attach various types of mutes to their horn. We hope that making our sensing apparatus no more difficult to attach and remove than a mute will facilitate adoption. Like the *Electrumpet* our design plans are available, the sensing apparatus is removable, and we utilize wireless communication. Our approach is more naturally integrated as it focuses on providing continuous control data from the positions of the three (3) valves used for playing. In contrast, the *Electrumpet* provides additional valve-like potentiometers and buttons that are not part of regular trumpet playing. The use of magnets and 3D printing for the housing is an additional difference and a contribution of our work. For sensing the continuous valve positions we utilize optical sensing, unlike the variable resistor potentiometers used in the *Electrumpet*. This optical sensing technique has been proposed in the design of another augmented trumpet which was done as a course project at Cornell University [4]. Unlike our approach it was used for discrete rather than continuous control. Figure 1 shows EROSS mounted on a trumpet.

2. MOTIVATION AND DESIGN

A long term objective of our research is to design and establish a robust, low cost, reconfigurable sensing hardware and software framework that can be adapted to various musical instruments in order to give them hyper-instrument capabilities without requiring invasive and hard to reverse modifications to the acoustic instrument. We believe that there is a strong need for such a framework because of the high cost and hard to replicate nature of existing hyperinstrument designs. Advances in open source software, electrical sensors, micro-controller frameworks such as Arduino [1], and 3D printing open the possibility of creating reusable, adaptable designs that can easily be applied to existing instruments without requiring extensive technical expertise and leveraging traditional playing technique. It is our hope that as electronics on stage are becoming more ubiquitous in many musical genres, approaches like ours will reach larger communities of users. The proposed trumpet sensing system is a good case study of how such a framework can be used for instrument augmentation.

2.1 Design Considerations

The proposed system, compared to other augmented trumpets that have been proposed, is minimal. It only provides continuous control information from the position of the three piston valves that are used for playing. This design decision was influenced by the designed principles for new musical interfaces outlined by Cook [2] that emphasize simplicity (*"Programmability is a curse"* and *"Smart instruments are often not smart"*) and integration with existing playing techniques (*"Copying an instrument is dumb, leveraging expert technique is smart"*). We also wanted the system design to be minimally invasive and easily removable for the reasons outlined above. The first one deals with the fact that the trumpet should remain physically unmodified, even not removing the valve bottom caps. These caps have a hole at the centre, which would work to our advantage. The location of the sensor would be such that the IR emitter would shoot a pulse through this hole and the reflection off the bottom surface of the piston would be detected by the photo-pin-diode. All trumpet pistons are hollow cylinders with cylindrical tunnels welded accross and an irregular bottom surface with a hole in its centre, which is concentric to the hole in the valve bottom cap. This configuration makes the optical path for the sensor multifaceted. When not pressed, the piston is at its maximum distance from the sensor and its bottom surface hole represent a small portion of the area covered by the sensor's detection zone. When fully pressed it is at the minimum distance from the sensor and the hole represent the majority, if not all, of the area covered by the detection zone, making it difficult to sense the appropriate distance to the piston's surface. Figure 2 depicts a valve's configuration and its interaction with the optical sensor.

Another challenge was the idea of having a system that could be easily attached and detached to the trumpet, but at the same time be sturdy enough to keep the sensors as steadily as possible beneath the valve's bottom cap. Optical sensors tend to have high sensitivity, and even the slightest of movements and/or temperature changes can affect the system's accuracy. To compensate for this issue a calibration stage needed to be included when designing the software. Also the system would have to be mounted in a way such that the performer shouldn't compromise his/her natural grasping technique.

[1] `http://www.arduino.cc`

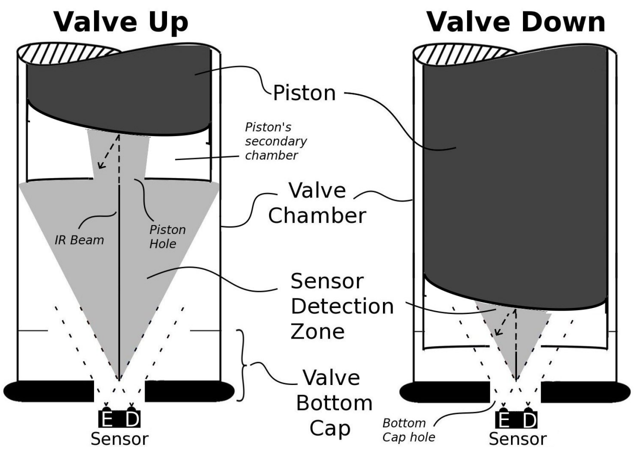

Figure 2: Issue with the sensor's detection zone

2.2 Sensor Placement

A critical aspect of the design is the placement of the optical sensors for determining the valve positions. In this section we describe the empirical investigation that was carried to determine this optimal placement according to a set of design constraints. Five candidate locations near the bottom cap were considered (indicated as $SL_1, \ldots, SL_5$ in Figure 3b). The optical sensor consists of an emitter and a detector. For each candidate location we collected the measured optical sensor readings for eight valve positions (indicated as $VP_1, \ldots, VP_8$ in Figure 3a). The full range of possible valve displacement was divided linearly into these eight valve positions where VP_1 is the fully released valve position and VP_8 is the fully pressed valve position.

The measured optical sensor readings are expected to be noisy. Thus to determine the best sensor placement, we need multiple measurements at each candidate location to obtain the noise distribution and a clear set of criteria by which to score each location.. We denote the vector of measurements for each configuration as

$$\mathbf{x}_l^p = x_l^p[1], \ldots, x_l^p[1000] \quad (1)$$

where $l = 1 \ldots 5$ corresponds to sensor location and $p = 1 \ldots 8$ corresponds to the valve positions. For each configuration of l, p we calculate the following statistics:

$$\mu_l^p = \frac{1}{N}\sum_{i=1}^{N} x_l^p[i] \quad (2)$$

$$\sigma_l^p = \sqrt{\frac{1}{N-1}\sum_{i=1}^{N}(x_l^p[i] - \mu_l^p)^2} \quad (3)$$

$$\rho_l^p = |\max(\mathbf{x}_l^p) - \min(\mathbf{x}_l^p)| \quad (4)$$

where $N = 1000$ in our case, μ is the sample mean, σ is the sample standard deviation, and ρ is the range. For each configuration we calculate the number of measurements C_l^p from $\mathbf{x}_l^p$ that fall within $\pm\sigma_l^p$ from the mean μ_l^p. Any configuration for which C_l^p was less than 70% was rejected.

Due to the complexity of the optical path, we used three (3) criteria to score the possible locations. The first one is Linearity, because it is desired that the system's transfer function (valve position vs. output data) is as linear as possible. The second one is Dynamic Range, to ensure a better signal-to-noise ratio. The third one is Robustness, because we want a location that robustly handles noise, such as the ones induced by the sensor and the mechanics of the system, providing consistent output measurements. A score was calculated for each criterion and each sensor location l.

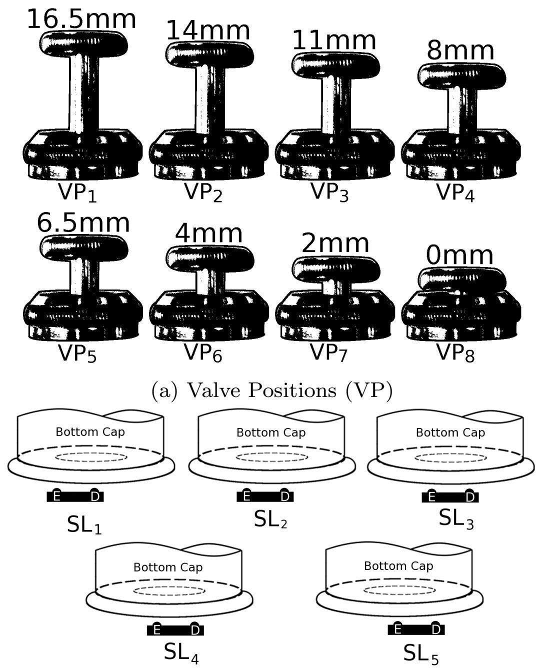

(a) Valve Positions (VP)

(b) Sensor Locations (SL)

Figure 3: Parameters for sensor placement analysis.

- **Linearity**

  The curve fitting cost L_l from a least squares linear fit on the means $\mu_l^{1,\ldots,8}$ of each VP instance corresponding to a particular location l (each curve is fitted to 8 points). Lower cost signifies a more linear response from the system.

- **Dynamic Range**

  The distance in measurement space between the minimum and maximum of two adjacent valve positions: $H_l^p = |\min(\mathbf{x}_l^p) - \max(\mathbf{x}_l^p)|$ where $p = 2, \ldots, 8$. To obtain a single score for a particular location l we weight each valve position with the following weights: $wh^p = [1.05, 1.15, 1.25, 1.35, 1.45, 1.55, 1.65]$. The weigths were determined empirically in order to emphasize the accuracy at the fully pressed position ($p = 8$). The final Dynamic Range score is $H_l = \sum_{p=2}^{8} wh^p \times H_l^p$. A higher score implies better dynamic range.

- **Robustness**

  The ratio $R_l^p = \sigma_l^p / \rho_l^p$ between the standard deviation and range for each configuration l, p (the d index is dropped based on the first experiment). As defined, this criteria is likely to be sensitive to outliners, but in fact this might work to our advantage because we are taking into account any possible noise, such as the one induced by the EROSS not being mechanically locked when mounted. To obtain a single robustness score for a particular location l we weight each valve position with the following weights: $wr^p = [1, 1.1, 1.2, 1.3, 1.4, 1.5, 1.6, 1.7]$. The final robustness score is $R_l = \sum_{p=1}^{8} wr^p \times R_l^p$. The weights were determined empirically in order to emphasize the accuracy at the fully pressed position ($p = 8$). A lower score implies better robustness.

The scores for the three most suitable sensor locations are in Table 1. These scores show that, while SL_4 is the more robust location, SL_1 has the least variation from a linear curve (Linearity criteria) and the wider dynamic range.

Table 1: Test results for critical valve position (Valve fully pressed)

Sensor Location	Linearity (L_l)	Dynamic Range (H_l^8)	Robustness (R_l^8)
SL_1	**752**	270	8
SL_4	2511	316	**6**
SL_5	1714	**402**	20

The scores R_l, H_l, L_l were normalized and added with equal weight to yield a final score S_l. The sensor location $\hat{l}$ that yielded the highest score $\hat{l} = \arg\max_l S_l$ was selected for the placing of the sensor and corresponds to the detector being positioned at the center, while the emitter sits at the edge, of the cap's hole (SL_1).

3. SYSTEM DESCRIPTION

The use of optical sensors provided the least invasive option out of different valve sensing approaches considered, such as the ones described in [13],[6]. Since the system is intended to perform range control on the trumpet valves rather than just event detection, a tightly focused sensor implementation was needed in order to achieve accurate results. As in previous work, the system's sensor location is at the bottom of the valves, below the bottom caps for easy retractability of the system. The system's main components are the optical sensors, the microcontroller and the wireless transceiver. All the details such as circuits schematics, part numbers, 3D models for the casing, software are available upon request.

Optical Sensors.

A fully integrated proximity sensor from Vishay[2] was chosen so the constraints on spatial resolution and robustness could be achieved. This sensor is a small surface mount device measuring 4mm (L) x 4mm (W) x 0.75 (H). It includes an IR emitter, photo-pin-diode and processing circuitry such that up to 16 bits of effective proximity resolution are possible. This sensor has an effective angle of half sensitivity of $\pm 55^\circ$, meaning that if we assume a cone-shaped detection zone with a $\pm 55^\circ$ angle (see Figure 2), then the intensity of radiation of the IR signal is at its maximum in the middle, and half the maximum on the edges. For proximity measurements, the emitter sends a train of pulses at a specific frequency and the detector, tuned to that same frequency, captures the reflected signal, which is subsequently processed and converted into the 16-bit output value, known as **counts**. The inherent noise from the circuitry is between ± 5 and ± 20 counts. It features an I^2C interface which is supported by the chosen microcontroller, and its performance features are configured by writing to registers in its internal processing unit.

Although it seem counterintuitive, the optimal location SL_1 allows for the IR signal within half of the detection zone to enter the valve chamber, while allowing full exposure of the detector to capture the reflected signal (see Figure 3b). Also, in principle this location ideally eliminates reflections off of the bottom cap. This is supported by the results from the analysis described in section 2.2.

Development Board.

A ready-made wireless development board developed by Texas Instruments (eZ430-RF2500)[3] was used. This package was chosen because of its immediate availability as well as ease of integration with the optical sensors via I^2C, plus the integrated wireless RF transceiver. Also, the fact that this board's size is 33mm (L) x 20mm (W) x 4mm (H) makes it more suitable for a minimally-invasive system. In addition, the microcontroller (MSP430F2274) in this board has some performance features that are relevant for this application. Perhaps the most important feature is the Low-Power mode (LPM), in which the microcontroller shuts down its CPU while in idle state (i.e. waiting for the user to press the activation button). Since the transmitter's side (Tx) is powered by a battery and not a power supply from the wall or a computer, this feature is very advantageous, as described in the section 4.3. It is also worth noting that the RAM size for this particular microcontroller is 1KB, so the system's software design had to be constrained by memory availability. The Flash memory size is 32KB and can be used when RAM is not available, however its slower performance must be taken into account.

3.1 Hardware Design

The system consists of three optical sensors located underneath the bottom valve caps connected via I^2C to the wireless development board.

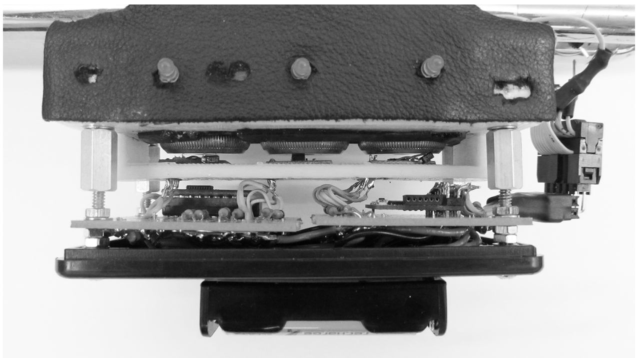

Figure 4: EROSS mounted under the valves

Unfortunately all three sensors come preprogrammed with a fixed slave address, which basically defeats the purpose of the I^2C protocol multi-drop capability. To overcome this issue an I^2C-based multiplexing device (TI's PCA9544A)[4] was incorporated into the design. An actuation button (SENSE), strategically attached to a trumpet valve guard so it doesn't interfere with the natural grasp of the instrument, gives the user control over the system to enable/disable sensing operation. Three (3) LED's (one for each valve) convey basic status information for the sensors. At the bottom part of the system the battery pack was attached, as well as an On/Off switch and a Calibration button (CAL). A removable mounting structure was 3D-printed using a Thing-O-Matic™ printer from MakerBot™. The structure consists of two (2) C-shaped sliding brackets coupled around the valve chambers for mechanical support. One bracket holds the circuit and sensors attached to the bottom, and the valve guard with the actuation button and status LED's attached to the side. The other bracket slides apart in order to detach the sensing apparatus. Figure 4 shows a close up picture of the mounted system and Figure 5 shows the 3D-printed mounting bracket with the attached sensors from a top view.

3.2 Software design

Due to the I^2C-bus' topography the sensing needed to be done sequentially. For the purpose of this system, the process of reading each sensor once is referred to as a **sensing cycle**. The transmitter's side of the system is the main component and its operation is described in this section.

[2]`http://www.vishay.com/docs/83798/vcnl4000.pdf`

[3]`http://www.ti.com/tool/ez430-rf2500`

[4]`http://www.ti.com/product/pca9544a`

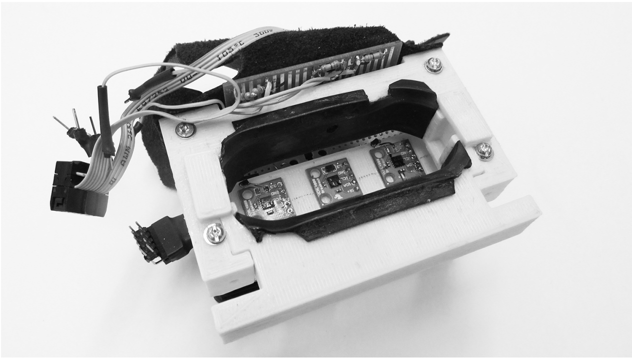

Figure 5: Top view of system housing

When powered-up, the microcontroller first makes sure the sensors are connected by testing the I^2C bus. Then it configures the sensors for proximity measurements by writing into the **IR LED current**; **Proximity Measurement Signal Frequency**; and **Proximity Modulator Timing Adjustment** registers. Once the sensors are initialized the system shuts down the CPU and waits for the user to press the **CAL** button. When the calibration (CAL) button is pressed the system goes into **Calibration** mode. In this mode the system performs ten (10) sensing cycles and averages the measurements. This process is done twice, one for the valves up to determine the lower boundary or **min**, and one for the valves down to determine the upper boundary or **max**. In this stage the slope of the linear model is calculated as:

$$m = \frac{1024}{max - min} \quad (5)$$

After calibration the CPU is shut down while it waits for the user to press the **SENSE** button. Due to the complexity of the optical path, there was a concern that there may not be a monotic relationship at the output (one value count for each position); and in that case it would be impossible to linearize the readings from the sensor, but in practice there was in fact a monotonic relationship. Linearization was done through the equation $Y = m(x - min)$, where x is the value from the sensor and Y is the linearized output value. m is the slope and min is the lower boundary, as calculated in the Calibration stage. In **Sensing** mode the system wirelessly transmits the linearized, averaged measurements from three sensing cycles. It stays in this mode until the system is powered-down again.

4. PERFORMANCE

Calibration is done everytime the system is powered-up and it compensates for any gain and offset error that the system may introduce. Main performance parameters are Spatial/Temporal resolution, System Robustness and Power Consumption.

4.1 Spatial / Temporal resolution

The trumpet valve has a range of 17mm (0.669”), and the optimal sensor position produces a full scale dynamic range of about 1000 counts or 10 bits, so the spatial resolution of $16.5\mu m$/value (micrometers per value). In practice we have found that there is a variation in full scale dynamic range across valves of 1-bit, possibly due to a variation in the reflective properties of the bottom of pistons. This small loss in resolution has minimal effect on practical performance. Latency is determined by the time it takes the system to read data from the sensors and send it over to the receiver. When using the microcontroller's Low-Power mode, the latency is 3.6 *msec*. The threshold for noticeable latency is 20 *msec* for the average human ear, but could go as low as 15 *msec*. This difference of 11.4 *msec* gives room to do more sensing cycles and average them, thus perhaps improving the robustness of the system. Operating the microcontroller in low-power mode has no significant effect on the latency.

Table 2: Estimated Battery-life time (hours).

	Idle		Sensing	
Type	LPM	no LPM	LPM	no LPM
AAA (700mAh)	170	94	77	78
LiPo (850mAh)	206	114	94	94

4.2 System Robustness

Under repeated trials involving attaching and detaching the current system, the greatest non-linearity transfer error, or variance, was of 15%, or about 150 counts in 1000 without averaging. Even though the robustness can be greatly improved by averaging the measurements and reducing the system's profile, it performs consistently after attaching/detaching. Time and usage would probably decrease the system's performance as the bottom of the pistons become less reflective, due to dust and spit. This issue is largely mitigated by the calibration stage.

4.3 Power Consumption

An estimation of the current drawn by the system would help determine the battery's life expectancy. For the first prototype two (2) rechargable AAA batteries with 700mAh of capacity were used; for the second implementation, a LiPo battery with a capacity of 850mAh was used. To estimate the battery's life cycle two (2) performance scenarios were studied: 1) **Idle**: After Initialization and Sensor Calibration, the system stays on but never goes into Sensing Operation mode. 2) **Sensing**: After Initialization and Sensor Calibration, the system goes into Sensing Operation mode and stays there until the battery is depleted. These two (2) scenarios cover the range of use of the system from minimum performance to full Sensing Operation. Two estimations were done, one with use of the microcontroller's Low-Power mode (LPM) and the other one without. Based on the results of Table 2, it is clear that the long battery life will ensure that changing or recharging batteries is infrequent.

5. IMPLEMENTATION & FUTURE WORK

The main goal of this paper is to describe the technical aspects of EROSS and motivate minimally invasive and easy to remove digital sensing systems for musical instruments in general. Therefore, we refrained from describing any explicit artistic mappings and performances with the system as we hope it can be used by many artists in different and unique ways.

In the curent configuration the added weight of EROSS (180*g* compared to the 880-1130g of a typical trumpet) still allows the trumpet to be held comfortably, but the high profile of the system, along with its low center of gravity affect the robustness of the EROSS by applying unwanted mechanical torque when tilting the trumpet. Replacing the AAA batteries with a slimmer LiPo battery, as well as designing a printed circuit board would reduce the system's profile, therefore reducing the torque and improving upon the robustness.

Future plans include providing versions of our system to other researchers experimenting with augmenting the trumpet as well as expert trumpet players that do not have a technical background. This way we can get feedback about how intuitive the system is to use, how stable and robust it is, what are possible improvements, as well as more subjective aspects such as whether or not it is inspiring to use, whether it hinders performance, and whether it fits into a particular artist's workflow. An easy to remove audio pickup in conjuction with real time pitch detection can be used to provide accurate pitch tracking information that can also be informed by the valve positions.

One interesting application of the proposed system that we are planning to explore is real-time transcription and latency compensation. This involves the concept of what we have been referring to as "Negative Latency". This concept is associated with the time it takes for the valve to go down when is pressed. In order to play a note, a trumpeter generally has the valve(s) already fully pressed down (open valve positions are a special case) when she/he starts to blow into the mouthpiece. From previous tests, it was determined that a player is able to fully press a valve in $50ms$. If the instant that he begins to blow is considered $t = 0ms$, because is when the sound is being produced, then at $t = -50ms$ he would have been starting to press the valve(s). This negative instant could be used to give the system a head start to perform calculations and predictions in effect compensating for any system induced latency. Based on a 90%-to-10% rise time (see Figure 6), characteristic of analog eletronics, the valve depression time is $30ms$. The idea is to study how this "Negative Latency" could improve time accuracy in real-time transcription, as opposed to more discrete approaches of valve sensing [3, 4].

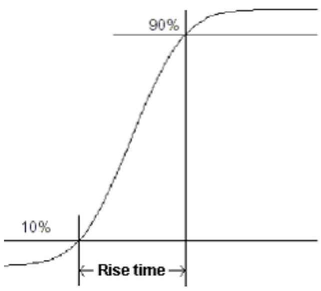

Figure 6: Rise time of an analog step function

6. CONCLUSIONS

Through this work, we aim to provide a low-cost and adaptable platform that artists can utilize without much background in engineering and electronics. This way they can realize their own specific vision while still taking advantage of a flexible framework for interactive physical computing. The use of minimally invasive and easy to remove augmentations to instruments has the potential to widen the adoption of hyperinstruments. We believe that EROSS demonstrates the potential of an easily removable, minimally invasive wireless sensing system for augmenting the trumpet with digital control capabilities.

Although in practice the dynamic range of the system is below the desired 10-bit range, it provides a fluid, dynamic and fairly linear response. The noise induced by the EROSS not being mechanically locked when mounted to the trumpet, plus the sensor's inherent noise, presented a decrease in the system's robustness. With a non-linearity measure of the system's transfer function in the order of 5%, it still proved to be robust enough to give consistent output when detaching and attaching the system. In summary, we have achieve our objectives of devising an easily removable system that provided continuous gesture control from the trumpet valves

The system was made possible by leveraging advances in sensors, micro-controllers, wireless transmission, and 3D printing. The system is stable and works as intended under the design constraints we posed. It does not affect acoustic trumpet playing and is tightly integrated with the gestures used for playing. We look forward to evolving our design for the trumpet as well as for other instruments. It is our hope that because of the open design of the system it will be adopted, used, and improved by others.

7. ACKNOWLEDGMENTS

Stephen Harrison, Duncan MacConnell, Dr. Eric Manning for their feedback and support in the development of this project. Ben Neill for inspiration. Dr. Mantis Cheng and Neill MacMillan for introducing us to the wonderful world of 3D printing. The UVic ECE Technical Support Staff (Brent Sirna, Paul Fedrigo, Rob Fitchner) for their wisdom. Lorena Mibelli for ongoing support.

8. REFERENCES

[1] M. Burtner. The metasaxophone: concept, implementation, and mapping strategies for a new computer music instrument. *Organised Sound*, 7(2):201–213, 2002.
[2] P. Cook. Principles for designing computer music controllers. In *Proc. Int. Conf. New Interfaces for Musical Expression (NIME)*, pages 1–4, 2001.
[3] P. Cook, D. Morrill, and J. Smith. A midi control and performance system for brass instruments. In *Proc. of the International Computer Music Conference (ICMC)*, pages 130–130, 1993.
[4] T. Craig and B. Factor. The trumpet midi controller. `http://courses.cit.cornell.edu/ee476/FinalProjects/s2008/twc22_bef23/twc22_bef23/index.html`.
[5] M. Davis. Live-evil. Music Album from Columbia Records, November 1971.
[6] A. Hollinger, J. Thibodeau, et al. An embedded hardware platform for fungible interfaces. In *Proc. the Int. Computer Music Conference (ICMC)*, pages 56–59, 2010.
[7] A. Kapur, A. Lazier, P. Davidson, R. Wilson, and P. Cook. The electronic sitar controller. In *Proc. Int. Conf. on New Interfaces for Musical Expression (NIME)*, pages 7–12, 2004.
[8] H. Leeuw. The electrumpet, a hybrid electro-acoustic instrument. In *Proc. Int. Conf. on New Interfaces for Musical Expression (NIME)*, 2009.
[9] T. Machover. *Hyperinstruments: A Progress Report, 1987-1991.* MIT Media Laboratory, 1992.
[10] B. Neill and B. Jones. Ben neill and bill jones: Posthorn. In *Proceedings of the 28th of the international conference extended abstracts on Human factors in computing systems*, pages 3107–3112. ACM, 2010.
[11] C. Palacio-Quintin et al. The hyper-flute. In *Proc. Int. Conf. New Interfaces for Musical Expression (NIME)*, 2003.
[12] J. Paradiso and N. Gershenfeld. Musical applications of electric field sensing. *Computer music journal*, 21(2):69–89, 1997.
[13] J. Thibodeau. Trumpet augmentation: Rebirth and symbiosis of an acoustic instrument. Master's thesis, McGill University, 2010.
[14] S. Trail, T. Fernandes, D. Godlovitch, and G. Tzanetakis. Direct and surrogate sensing for the gyil african xylophone. In *Proc. Int. Conf. New Interfaces for Musical Expression (NIME)*, 2012.